

See discussions, stats, and author profiles for this publication at: <https://www.researchgate.net/publication/13282666>

# Thermodynamic properties of $S = 1$ antiferromagnetic Heisenberg chains as Haldane systems

Article in *Physical review. B, Condensed matter* · November 1993

DOI: 10.1103/PhysRevB.48.9528 · Source: PubMed

CITATIONS

70

READS

63

2 authors:



**Shoji Yamamoto**

Hokkaido University

146 PUBLICATIONS 2,465 CITATIONS

[SEE PROFILE](#)



**Seiji Miyashita**

The University of Tokyo

383 PUBLICATIONS 8,147 CITATIONS

[SEE PROFILE](#)

Some of the authors of this publication are also working on these related projects:



photoinduced phase transition [View project](#)



modified spin-wave theory [View project](#)

# Thermodynamic properties of $S = 1$ antiferromagnetic Heisenberg chains as Haldane systems

Shoji Yamamoto

*Department of Physics, College of General Education, Osaka University, Toyonaka, Osaka 560, Japan*

Seiji Miyashita

*Graduate School of Human and Environmental Studies, Kyoto University, Kyoto 606, Japan*

(Received 3 May 1993)

Thermodynamic properties of  $S = 1$  antiferromagnetic Heisenberg chains with free and periodic boundaries are investigated by a quantum Monte Carlo method. In particular, temperature dependences of the specific heat, the magnetic susceptibility, and the hidden order parameter, which are inherent to the Haldane phase, are investigated. The specific heat turns out to have a peak at a temperature  $T_{\text{peak}} \sim 2\Delta$ , where  $\Delta$  is the energy gap of the present model, although the temperature dependence of the specific heat is very similar to the Schottky type. In open chains, due to the fourfold degeneracy of the ground state, the magnetic susceptibility shows a Curie-like divergence regardless of the number of spins in the chain. The amplitude of the Curie-like divergence is consistent with the edge moments ( $S = \frac{1}{2}$ ). On the other hand, it is confirmed that the long-range hidden order exists only in the ground state. How the hidden order grows as the temperature goes to zero ( $T \rightarrow 0$ ) is investigated by introducing an intrinsic correlation length  $\xi_D$  of the ordering, which diverges as  $T \rightarrow 0$ . A qualitative difference in fluctuations between the ground state and the finite-temperature states is discussed making use of snapshots of the transformed two-dimensional Ising system on which a Monte Carlo simulation is being performed.

## I. INTRODUCTION

Haldane predicted<sup>1</sup> in 1983 that antiferromagnetic Heisenberg chains have an energy gap between the ground state and the first excited state and the spin-correlation function in the ground state decays exponentially for the integer spin cases in contrast with the cases of half-odd integer spin. Since then, low-temperature properties of the  $S = 1$  antiferromagnetic Heisenberg chain have been vigorously studied. The existence of the gap was theoretically confirmed in fact by a numerical diagonalization method,<sup>2</sup> a transfer-matrix method,<sup>3</sup> and various Monte Carlo methods.<sup>4</sup> The gap was also observed experimentally.<sup>5,6</sup> The exponential decay of the spin-correlation function was confirmed mainly by Monte Carlo simulations.<sup>7</sup> On the other hand, various analytical approaches have clarified the mechanism of these phenomena. Affleck and Lieb made clear the difference between integer spin and half-odd integer spin systems and discussed the origin of the gap,<sup>8</sup> as well as the existence of the gap itself. Affleck, Kennedy, Lieb, and Tasaki (AKLT) introduced an exactly solvable model<sup>9</sup> which has the typical nature predicted by Haldane and clarified the underlying physical mechanism of these phenomena.

The ground state has turned out to have peculiar properties. In spite of the exponential decay of the correlations, den Nijs and Rommelse pointed out<sup>10</sup> that there is an antiferromagnetic hidden order; that is, the antiferromagnetic alignment of  $\pm 1$  spins after omitting all the sites with spin projection 0. To detect this hidden order they introduced a nonlocal string order parameter,

$$O_{\text{string}}^z = \lim_{L \rightarrow \infty} O_{\text{string}}^z(L), \quad (1)$$

where

$$O_{\text{string}}^z(L) = -S_1^z \exp \left[ i\pi \sum_{j=2}^{L-1} S_j^z \right] S_L^z. \quad (2)$$

Their string order parameter, which takes a full value of 1 in the ground state of the AKLT model,<sup>9</sup> was numerically evaluated<sup>11</sup> and confirmed to be nonzero in the ground state of the usual  $S = 1$  Heisenberg model. Tasaki has tried another approach<sup>12</sup> to the hidden symmetry described by the string order (1) and Kennedy and Tasaki have theoretically developed a picture of the hidden symmetry.<sup>13</sup> Mikeska has clarified the nature of the Haldane phase making use of a transformed  $S = \frac{1}{2}$  system.<sup>14</sup> One of the main aims of the present paper is to clarify the size and temperature dependences of the nonlocal hidden order detected by the order parameter (1). The string order parameter of den Nijs and Rommelse is equal with the following nonlocal (long-range) order parameter,

$$O_{\text{LR}} = \left[ \sum_{i=1}^L (-1)^{\sum_{j=1}^i |S_j^z|} S_i^z \right] / \left[ \sum_{i=1}^L |S_i^z| \right]. \quad (3)$$

We calculate  $\langle O_{\text{LR}}^2 \rangle$  at various chain lengths  $L$  and over a wide range of temperature and obtain  $\lim_{L \rightarrow \infty} \langle O_{\text{LR}}^2 \rangle$  by extrapolating them. Here  $\langle \cdots \rangle$  denotes a thermal average of the quantity at a given temperature. As a result, we have found that  $\langle O_{\text{LR}}^2 \rangle$  shows a strong  $L$  dependence at finite temperatures and  $\langle O_{\text{LR}}^2 \rangle \rightarrow 0$  as  $L \rightarrow \infty$ . On the other hand, we have confirmed that  $\langle O_{\text{LR}}^2 \rangle$  has a nonzero value only in the ground state.

Besides the nonlocal string order parameter, we introduce the following quantity to describe the local property of the hidden order. At first we omit all the sites with

spin projection 0 and after that we denote the nearest spin pairs aligned antiferromagnetically and ferromagnetically by  $(\pm\mp)$  and  $(\pm\pm)$ , respectively. Then the local (short-range) hidden order parameter for a  $L$ -site chain is defined by

$$O_{\text{SR}} = \frac{N(\pm\mp) - N(\pm\pm)}{N(\pm\mp) + N(\pm\pm)}, \quad (4)$$

where  $N(\cdots)$  is the total number of the nearest spin pairs of  $(\cdots)$  type in the hidden ordering. It should be noted that the pair  $(\pm\pm)$  can be regarded as a domain wall breaking the nonlocal hidden order. Recently, based on a study of the ground states with various boundary conditions, Sakai has proposed<sup>15</sup> that these domain walls have a formation energy which is equal to the energy gap. In this sense the order parameter (4) can be considered to be the effective energy of the system. We have found that  $\langle O_{\text{SR}} \rangle$  is weakly dependent on the chain length  $L$  and has a temperature dependence similar to that of the energy.

Since fourfold degeneracy of the ground state and appearance of two effective spin  $\frac{1}{2}$ 's at edges were found in the AKLT model with the free boundary condition,<sup>9</sup> much attention had been paid to the properties of open chains. Kennedy has found<sup>16</sup> that these properties of the ground state in open chains are also observed in certain kinds of models including the usual  $S=1$  Heisenberg model. The present authors have performed Monte Carlo simulations<sup>17</sup> for open chains with up to 97 spins and have confirmed in long enough chains the fourfold degeneracy of the ground state in open chains and the appearance of the localized  $\frac{1}{2}$  magnetic moments at edges, i.e., the Kennedy conclusion. In particular, they explicitly studied the size dependence of the low-lying energy levels and visualized the spatial distribution of the staggered magnetic moments which has been also obtained by a renormalization-group method.<sup>18</sup> The edge moments of  $S=\frac{1}{2}$  were also observed experimentally<sup>19</sup> in open chains separated by not only magnetic but also nonmagnetic ions.

In spite of the extensive studies of the ground-state properties, the finite-temperature properties have not been well reported yet. In the present paper, we calculate the energy, the specific heat, and the magnetic susceptibility, as well as the above-introduced hidden order parameters. Concerning the specific heat, the data have already been obtained by other methods. Long before the Haldane conjecture, Blöte had calculated the specific heat of magnetic linear chains for  $S=1$  to  $\frac{5}{2}$  by a numerical diagonalization method.<sup>20</sup> Betsuyaku and Yokota applied a transfer-matrix method to the  $S=1$  Heisenberg model and obtained the energy and the specific heat.<sup>21</sup> Kubo also calculated the energy by a transfer-matrix method.<sup>22</sup> However, in their work, they discussed neither the effects of the system size and the boundary condition on the specific heat nor the temperature dependence of the specific heat in connection with the Haldane gap. Thus, here we also show the data for the specific heat of finite chains with the free and periodic boundary conditions where the structure of the low-lying energy levels in the

Haldane phase are different. As for the magnetic susceptibility, the Curie-like divergence attributed to the edge moments has been observed experimentally.<sup>23</sup> Our Monte Carlo simulations have also confirmed that as the temperature goes to zero ( $T \rightarrow 0$ ), the magnetic susceptibility shows the Curie-like divergence in open chains with not only odd but also even numbers of spins, while it converges to zero in periodic chains. We have further found that the amplitude of the divergence is consistent with two effective spin  $\frac{1}{2}$ 's, rather than a single spin 1.

In Sec. II we explain the model and method. We show the data for the energy and the specific heat in Sec. III, the magnetic susceptibility in Sec. IV, and the hidden orders in Sec. V. Section VI is devoted to summary and discussion.

## II. MODEL AND METHOD

We study  $S=1$  Heisenberg chains described by the Hamiltonian,

$$\mathcal{H} = \sum_{i=1}^L J_i \mathbf{S}_i \cdot \mathbf{S}_{i+1} \equiv \sum_{i=1}^L V_i, \quad (5)$$

where  $L$  is the number of spins and  $\mathbf{S}_{L+1} = \mathbf{S}_1$ . In the present article we consider antiferromagnetic chains of three types, namely, open chains with odd and even numbers of spins (open odd and even chains) and periodic chains with even numbers of spins. In each case the exchange interaction  $J_i$  in Eq. (5) is given as follows:

$$J_i = J \quad (i=1, 2, \dots, L-1), \quad J_L = 0, \quad (6)$$

for open chains, and

$$J_i = J \quad (i=1, 2, \dots, L) \quad (7)$$

for periodic chains.

Using the Suzuki-Trotter decomposition<sup>24</sup> of checkerboard-type,<sup>25</sup> we obtain the following equation for the partition function  $Z$ :

$$Z \simeq \text{Tr}[(e^{-\beta \mathcal{H}_A/n} e^{-\beta \mathcal{H}_B/n})^n], \quad (8)$$

where  $\beta = (k_B T)^{-1}$  with the Boltzmann constant  $k_B$  and

$$\mathcal{H}_A = \sum_{i=1,3,\dots} V_i, \quad \mathcal{H}_B = \sum_{i=2,4,\dots} V_i. \quad (9)$$

Monte Carlo simulations are performed on a transformed two-dimensional  $S=1$  Ising system with four-body interactions corresponding to the local Boltzmann factor (Fig. 1),

$$\rho_{i,r} = \langle S_{i,r} S_{i+1,r} | e^{-\beta V_i/n} | S_{i,r+1} S_{i+1,r+1} \rangle, \quad (10)$$

where  $S_{i,r}$  takes  $\pm 1$  and 0, and  $r$  is a label along the Trotter direction. Monte Carlo flips are performed keeping the conservation law of the magnetization in shaded plaquettes as shown in Fig. 1,

$$S_{i,r} + S_{i+1,r} = S_{i,r+1} + S_{i+1,r+1}. \quad (11)$$

The Trotter number  $n$  should, in principle, be taken to be as large as possible. However, the spin configuration gets hard to change as the quantity  $\beta/n$  becomes too

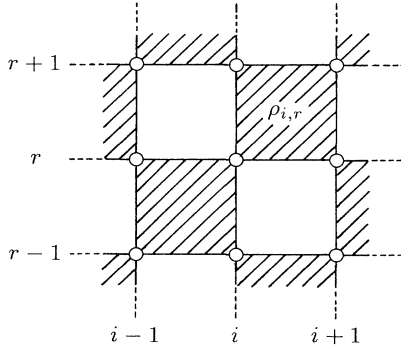


FIG. 1. Graphical representation of the transformed two-dimensional Ising system, where shaded plaquettes represent the local Boltzmann factors.

small.<sup>26</sup> On the other hand, global flips to change the total magnetization, namely, the flips along the Trotter direction, are hard to be accepted at low temperatures. Consequently, many Monte Carlo steps are needed to equilibrate the system at a large  $n$  and a low temperature. Thus, according to temperature, we have used different sets of Trotter numbers and have performed different numbers of Monte Carlo steps. We list in Table I the used Trotter numbers and the performed Monte Carlo steps for a Trotter number at each temperature. In all the cases, the first  $2 \times 10^4$  Monte Carlo steps were discarded as the initial transient stage for thermalization. The  $n$  dependence is extrapolated by the least-squares method using the formula

$$A(n) = A_\infty + \frac{A_1}{n^2} + \frac{A_2}{n^4}. \quad (12)$$

For high temperatures  $k_B T/J = 3.0 \sim 5.0$ , only a single Trotter number was taken and the extrapolation was not performed.

TABLE I. The used Trotter numbers ( $n$ ) and the performed Monte Carlo steps (MCS) for a Trotter number at given temperatures ( $T$ ).

$k_B T/J$	$n$	MCS
0.15	8,12,16,24	$32 \times 10^4$
0.20	6,8,12,16	$32 \times 10^4$
0.30	4,6,8,12	$27 \times 10^4$
0.40	4,6,8,12	$27 \times 10^4$
0.60	4,6,8,12	$17 \times 10^4$
0.80	4,6,8,12	$17 \times 10^4$
1.00	4,6,8,12	$17 \times 10^4$
1.20	2,4,6,8	$17 \times 10^4$
1.40	2,4,6,8	$17 \times 10^4$
1.60	2,4,6,8	$17 \times 10^4$
1.80	2,4,6,8	$17 \times 10^4$
2.00	2,4,6,8	$17 \times 10^4$
3.00	4	$14 \times 10^4$
4.00	4	$14 \times 10^4$
5.00	4	$14 \times 10^4$

The precision in data depends on both the physical quantity and temperature and is, on the whole, between three and two digits. In Monte Carlo simulations, the energy can be rather easily evaluated with accuracy, while it is generally hard to evaluate precisely the specific heat and the magnetic susceptibility at low temperatures. Thus the specific heat is also calculated as a numerical derivative of the energy. The formula for the energy  $E$  and the specific heat  $C$  are<sup>27</sup>

$$E = -\langle Q_1 \rangle_{\text{MC}}, \quad (13)$$

$$C = \frac{1}{k_B T^2} (\langle Q_1^2 \rangle_{\text{MC}} - \langle Q_1 \rangle_{\text{MC}}^2 + \langle Q_2 \rangle_{\text{MC}}), \quad (14)$$

where

$$\left. \begin{aligned} Q_1 &= \sum_{i,r} \left[ \frac{\partial \rho_{i,r}}{\partial \beta} / \rho_{i,r} \right], \\ Q_2 &= \sum_{i,r} \left[ \frac{\partial^2 \rho_{i,r}}{\partial \beta^2} / \rho_{i,r} - \left( \frac{\partial \rho_{i,r}}{\partial \beta} / \rho_{i,r} \right)^2 \right] \end{aligned} \right\} \quad (15)$$

and  $\langle \cdots \rangle_{\text{MC}}$  denotes the Monte Carlo average of the quantity at a given temperature  $T$ . Here we have obtained the specific heat directly through Eq. (14) and also from the temperature derivative of the energy.

### III. ENERGY AND SPECIFIC HEAT

We show in Fig. 2 the temperature dependences of the energy in open odd chains (a) and periodic chains (b). The data for open even chains are very similar to those for open odd chains. The symbols  $\square$  in Fig. 2(b) denote the data obtained by a transfer-matrix method<sup>21,22</sup> and give good agreement with the present results. Although a weak size dependence is observed in open chains, open and periodic chains show exactly the same behavior in the thermodynamic limit.

Figure 3 shows the temperature dependences of the specific heat in open odd chains (a) and periodic chains (b) calculated directly through Eq. (14). There is no essential difference between the results for open odd and even chains, as is expected from the energy results for them. We also show in Fig. 4 the temperature dependence of the specific heat in open odd chains obtained by differentiating the energy numerically with respect to temperature. The symbols  $\square$  in Fig. 3(b) denote the data obtained by an exact diagonalization method<sup>20</sup> and give good agreement with the present results. Figures 3 and 4 must show exactly the same behavior. However, the directly obtained data show poor convergence at low temperatures. Thus, in the case of calculating the specific heat, it is better to obtain the data from the temperature derivative of the energy at low temperatures, while, at higher temperatures, it is better to evaluate the values directly without calculating the energy at many temperature points.

Although the low-lying energy spectra are qualitatively different in open and periodic chains,<sup>9,16</sup> the specific heat has turned out to have similar shapes for them even in

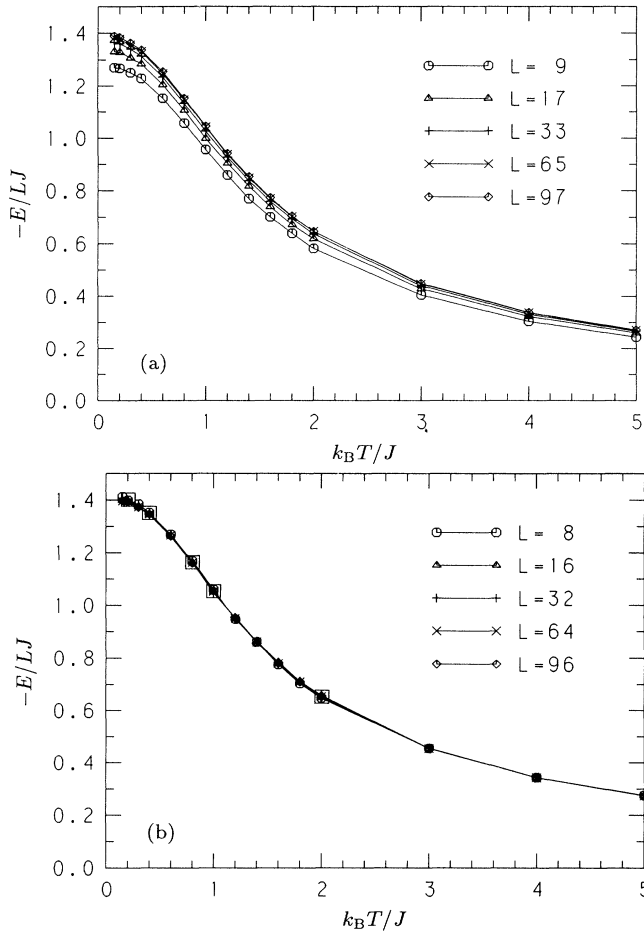


FIG. 2. Temperature dependences of the energy per spin in open chains with odd numbers of spins (a) and periodic chains (b). The symbols  $\square$  in (b) denote the data obtained by a transfer-matrix method (Refs. 21 and 22).

the cases of finite chain length. Furthermore, it should be noted that although the temperature dependence is very similar to the Schottky-type specific heat, the peak temperature is about  $0.8J \sim 2\Delta$ , where  $\Delta$  is the energy gap of the present model. We note that the peak of the specific heat of the Schottky type is located at  $0.42\Delta_0$ , where  $\Delta_0$  is the corresponding energy difference. From these facts, it is concluded that the temperature dependence of the specific heat should not be attributed to the energy gap between the ground state and the first excited state in the present case. Therefore, we should be prudent in estimating the coupling constant  $J$  from the experimentally observed specific heat.

#### IV. MAGNETIC SUSCEPTIBILITY

We show in Fig. 5 the temperature dependences of the magnetic susceptibility per spin  $\chi^L/L$  in open odd chains (a), open even chains (b), and periodic chains (c), where

$$\chi^L = \frac{1}{T} \left[ \left\langle \left( \sum_{i=1}^L S_i^z \right)^2 \right\rangle - \left\langle \sum_{i=1}^L S_i^z \right\rangle^2 \right]. \quad (16)$$

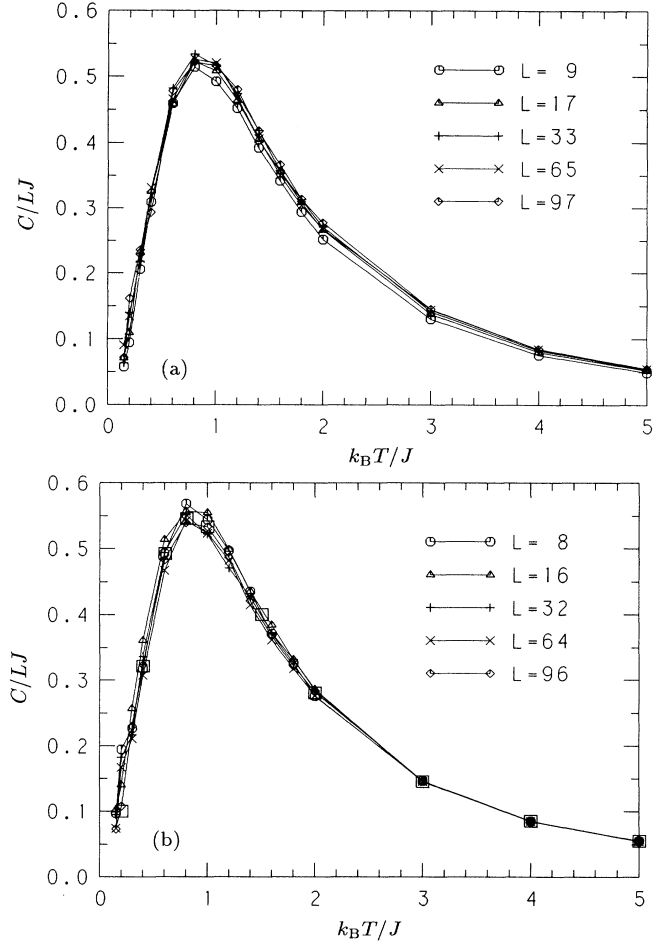


FIG. 3. Temperature dependences of the specific heat per spin in open chains with odd numbers of spins (a) and periodic chains (b) calculated directly through Eq. (14) (see text). The symbols  $\square$  in (b) denote the data obtained by an exact diagonalization method (Ref. 20).

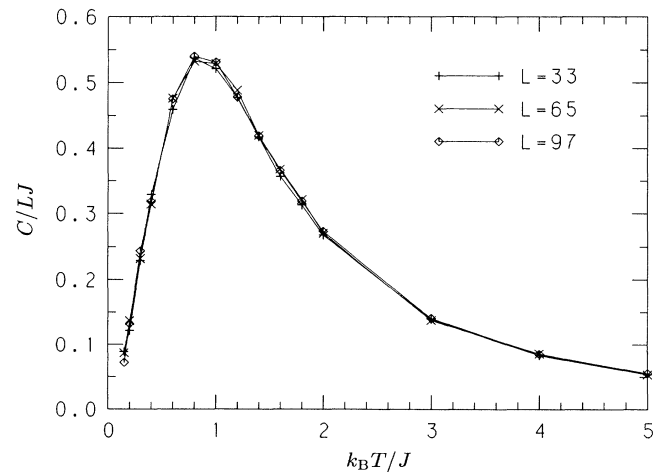


FIG. 4. Temperature dependences of the specific heat per spin in open chains with odd numbers of spins (a) and periodic chains (b) obtained by differentiating the energy numerically with respect to temperature.

In open chains a Curie-like divergence is observed as  $T \rightarrow 0$ , while in periodic chains the susceptibility vanishes at  $T=0$ . The divergence in the present model is attributed to the fourfold degeneracy of the ground state in open chains which are the inherent phenomena in the Haldane

systems. More explicitly, the two effective spin  $\frac{1}{2}$ 's induced in the boundaries bear the divergence. Thus, in the present model, the divergence is observed not only in open odd chains but also in open even chains. However, a careful observation shows us a quantitative difference in the diverging behavior between open odd and even chains at small  $L$ 's, where the fourfold degeneracy is not exact. The four lowest eigenvalues consist of the lowest triplet levels and the singlet level slightly above them in open odd chains, while in open even chains they consist of the lowest singlet level and the triplet levels slightly above it. The separation of these eigenvalues exponentially converges to zero when the chain length goes to infinity.<sup>16,17</sup> However, the fourfold degeneracy can be practically realized for  $L > 16$  and consequently, we can clearly observe the difference between odd and even chains only in the cases of  $L=9$  and  $8$  [Figs. 5(a) and 5(b)].

Let us analyze quantitatively the Curie-like divergence. The diverging part can be extracted by subtracting the bulk susceptibility which is estimated from periodic chains,

$$\chi_{\text{Curie}} \simeq \chi_{\text{open}}^L - \chi_{\text{periodic}}^{L-1}. \quad (17)$$

We show in Fig. 6 the temperature dependence of  $\chi_{\text{Curie}}$ . Although the curves for long chains show a jagged behavior, we observe the  $L$ -independent behavior of  $\chi_{\text{Curie}}$ . The amplitude of the divergence is estimated as

$$\chi_{\text{Curie}} \simeq \frac{0.5}{T}. \quad (18)$$

This amplitude is consistent with the Curie divergence owing to the two magnetic moments of  $S=\frac{1}{2}$  at edges,  $2(\frac{1}{3})[S(S+1)/T]_{S=1/2}$ . A single moment of  $S=1$  would cause the divergence,

$$\chi_{\text{Curie}} = \left[ \frac{S(S+1)}{3T} \right]_{S=1} = \frac{2}{3T}. \quad (19)$$

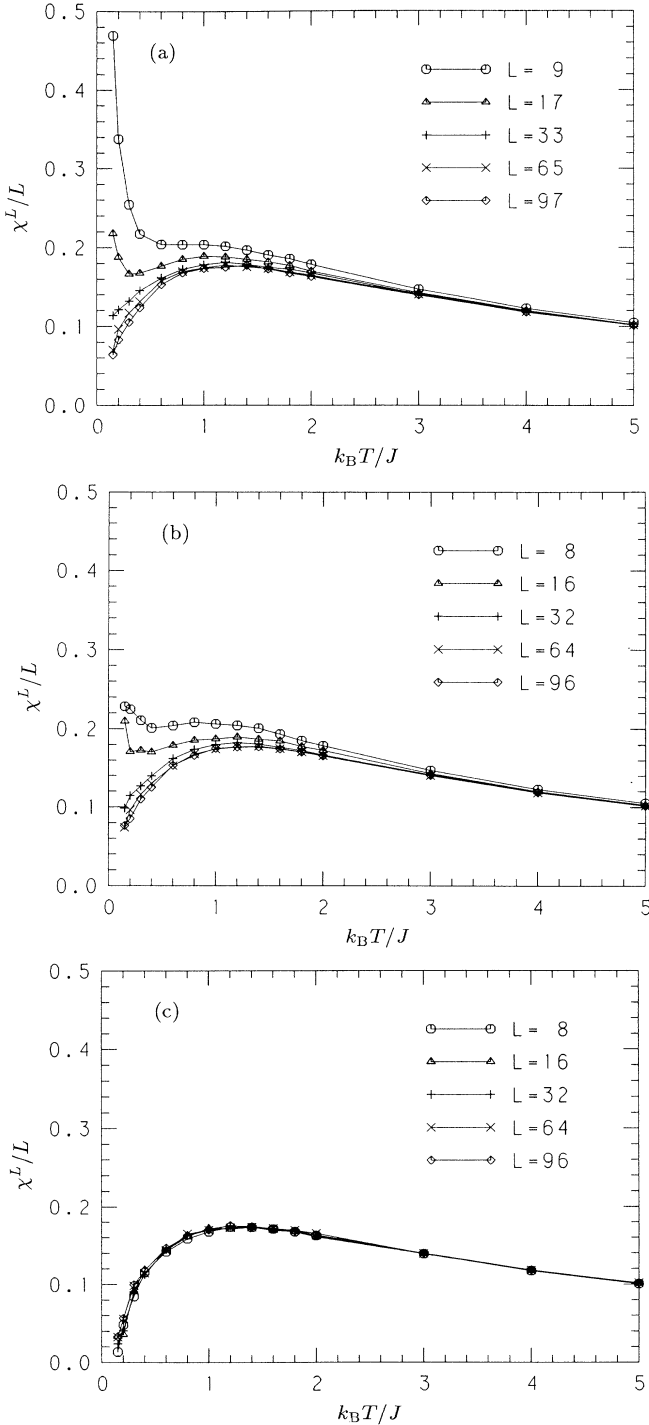


FIG. 5. Temperature dependences of the magnetic susceptibility per spin in open chains with odd (a) and even (b) numbers of spins and periodic chains (c).

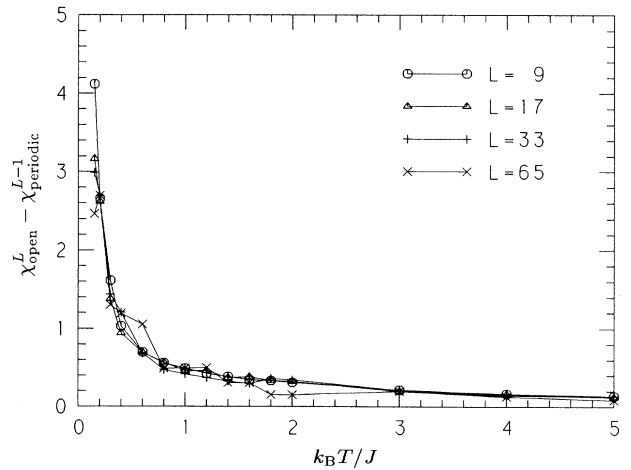


FIG. 6. Curie-like divergence of the magnetic susceptibility in open chains with odd numbers of spins. See Eq. (19) in the text.

Using the present result, we can estimate the number of open chains in a sample. Figure 5 reproduces in fact the experimentally observed behavior of the magnetic susceptibility.<sup>23</sup>

### V. HIDDEN ORDER

One of the most inherent properties found in the Haldane phase is the existence of the hidden order which has been mentioned in Sec. I. We show in Fig. 7, a snapshot of the transformed two-dimensional Ising system at a very low temperature at which a Monte Carlo simulation is being performed, where the horizontal and vertical lines denote the chain and Trotter directions, respectively. The hidden order, namely, the antiferromagnetic alignment of  $\pm 1$  spins with several spin projection 0 between them is observed. It is well known that in the AKLT model a perfect hidden order appears in the ground state. However, local destructions of the order are observed in the snapshot, although the temperature of the snapshot is low enough to obtain the ground-state properties. In Fig. 7 we have encircled with lines the antiphase domains which have the phase opposite to the background. In the present model, the hidden order is locally broken by quantum fluctuations. In this section we quantitatively study the hidden order with the order parameters of two types,  $O_{\text{SR}}$  and  $O_{\text{LR}}$ , introduced in Sec. I. Let us rewrite  $O_{\text{SR}}$  and  $O_{\text{LR}}$  as

$$O_{\text{SR}} = \begin{cases} -\sum_{i=1}^{\tilde{L}-1} \tilde{S}_i^z \tilde{S}_{i+1}^z / \sum_{i=1}^{\tilde{L}-1} |\tilde{S}_i^z \tilde{S}_{i+1}^z|, & \text{for open chains,} \\ -\sum_{i=1}^{\tilde{L}} \tilde{S}_i^z \tilde{S}_{i+1}^z / \sum_{i=1}^{\tilde{L}} |\tilde{S}_i^z \tilde{S}_{i+1}^z|, & \text{for periodic chains,} \end{cases} \quad (20)$$

$$O_{\text{LR}} = \frac{1}{\tilde{L}} \sum_{i=1}^{\tilde{L}} (-1)^i \tilde{S}_i^z, \quad (21)$$

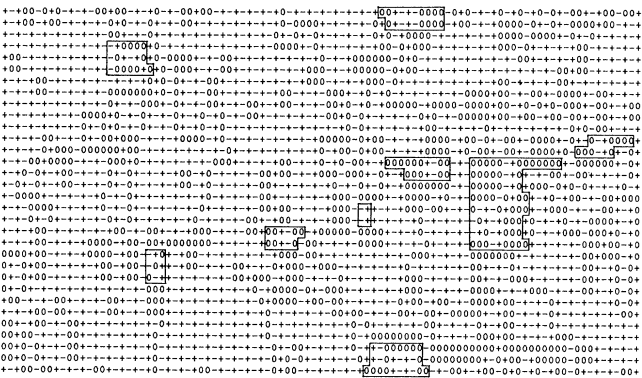


FIG. 7. A snapshot of the transformed two-dimensional Ising system on which a Monte Carlo simulation is being performed, where the horizontal and vertical lines denote the chain and Trotter directions corresponding to space and time, respectively. Here  $k_B T/J=0.1$ , and it can be regarded to be small enough to obtain the ground-state properties.

where  $\{\tilde{S}_1^z, \tilde{S}_2^z, \dots, \tilde{S}_{\tilde{L}}^z\}$  is a sequence of nonzero spins in an  $L$ -site chain,  $\tilde{L}$  is the number of nonzero spins in the chain, and  $\tilde{S}_{\tilde{L}+1}^z = \tilde{S}_1^z$ .

Since  $\tilde{S}_i^z \tilde{S}_{i+1}^z = \pm 1$ , the probability to have a domain wall in the hidden ordering at each pair,  $P_{\text{DW}}$ , is given by  $O_{\text{SR}}$  as

$$P_{\text{DW}} = \frac{1}{2}(1 - O_{\text{SR}}). \quad (22)$$

In the ground state of the AKLT model,  $\langle O_{\text{SR}} \rangle = 1$ , that is, there is no probability of the domain wall. We show in Fig. 8 the temperature dependences of  $\langle O_{\text{SR}} \rangle$  in open odd chains (a) and periodic chains (b). The general tendency of the temperature and size dependences of  $\langle O_{\text{SR}} \rangle$  is similar to that of the energy (Fig. 2), which suggests that the domain walls in the hidden order have an important role in the energy structure of the system. But as we mentioned in Sec. III, the present model cannot be re-

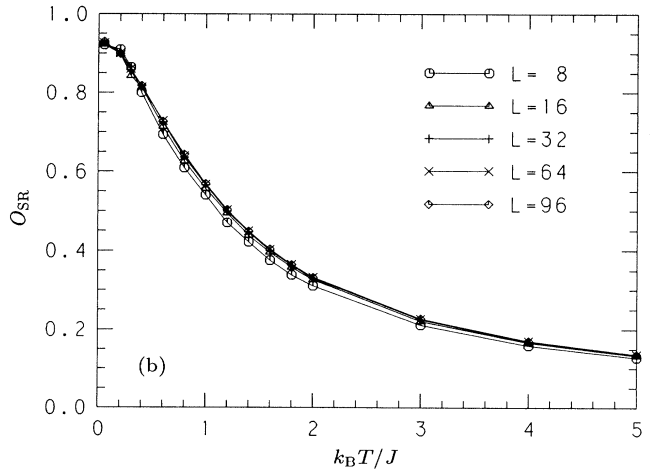
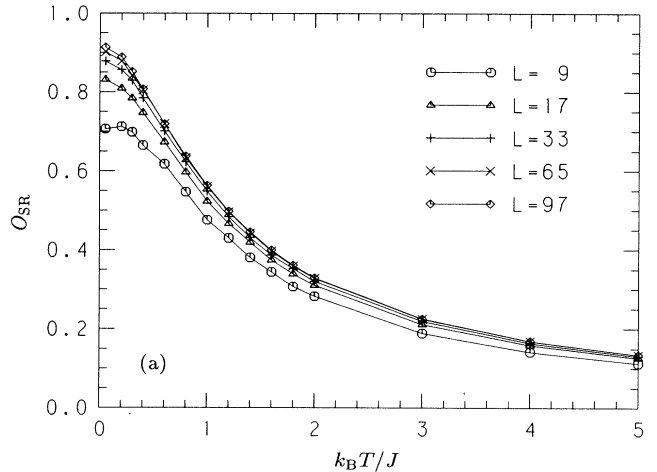


FIG. 8. Temperature dependences of the local (short-range) hidden order parameter in open chains with odd numbers of spins (a) and periodic chains (b). Here the data at  $k_B T/J=0.05$  have been estimated through Eqs. (27) and (28), using the corresponding values obtained in the canonical ensemble where the total magnetization  $M_z$  is fixed.

garded as a simple two-level system. It is found that the temperature derivative of  $\langle O_{\text{SR}} \rangle$  has a peak around  $k_B T/J=0.4$ , while the energy has a peak around  $k_B T/J=0.8$ . Detailed analysis of the relation between the energy and  $O_{\text{SR}}$  will be investigated elsewhere.

The nonlocal hidden order has been extensively studied and several types of order parameters were introduced to detect the order.<sup>28</sup> In order to investigate the quantity  $O_{\text{LR}}$  given in Eq. (21), we have observed  $\langle O_{\text{LR}}^2 \rangle$ , which can be represented in the system with translation symmetry as

$$O_{\text{LR}}^2 = \frac{1}{\tilde{L}} \sum_{i=1}^{\tilde{L}} (-1)^{i+1} \tilde{S}_i^z \tilde{S}_i^z = \frac{1}{\tilde{L}} \sum_{i=1}^{\tilde{L}} O_{\text{string}}^z(\hat{i}), \quad (23)$$

where  $\hat{i}$  is the original position of  $\tilde{S}_i^z$  in the chain. Generally, the definition of the length in the nonzero spin system  $\{\tilde{S}_i^z\}$  is different from the original length of the chain. But if we assume that  $S=0$  appears uniformly on

the chain, the former length is considered to be  $\frac{2}{3}$  of the original chain length. In the ground state of the AKLT model,  $\langle O_{\text{LR}}^2 \rangle = 1$ ; while in the present model, the value of  $\langle O_{\text{LR}}^2 \rangle$  is reduced to less than unity even at  $T=0$ . At finite temperatures,  $\langle (-1)^{i+1} \tilde{S}_i^z \tilde{S}_i^z \rangle$  decays exponentially. Let us denote the correlation length of the decay by  $\xi_D$ . From Eq. (23) we expect that

$$\langle O_{\text{LR}}^2 \rangle \propto \frac{1}{\tilde{L}} \int_0^{\tilde{L}} e^{-r/\xi_D} dr \simeq \frac{\xi_D}{\tilde{L}}, \quad (24)$$

for  $\tilde{L} > \xi_D$ . Thus  $\langle O_{\text{LR}}^2 \rangle$  is expected to be proportional to  $L^{-1}$  and in the thermodynamic limit,  $\langle O_{\text{LR}}^2 \rangle = 0$  unless  $\xi_D$  diverges. We show in Fig. 9 the temperature dependences of  $\langle O_{\text{LR}}^2 \rangle$  in open odd chains (a) and periodic chains (b). In contrast to the local hidden order (Fig. 8), the nonlocal hidden order has a strong size dependence. To observe this dependence more quantitatively we also show in Fig. 10 the size dependences of

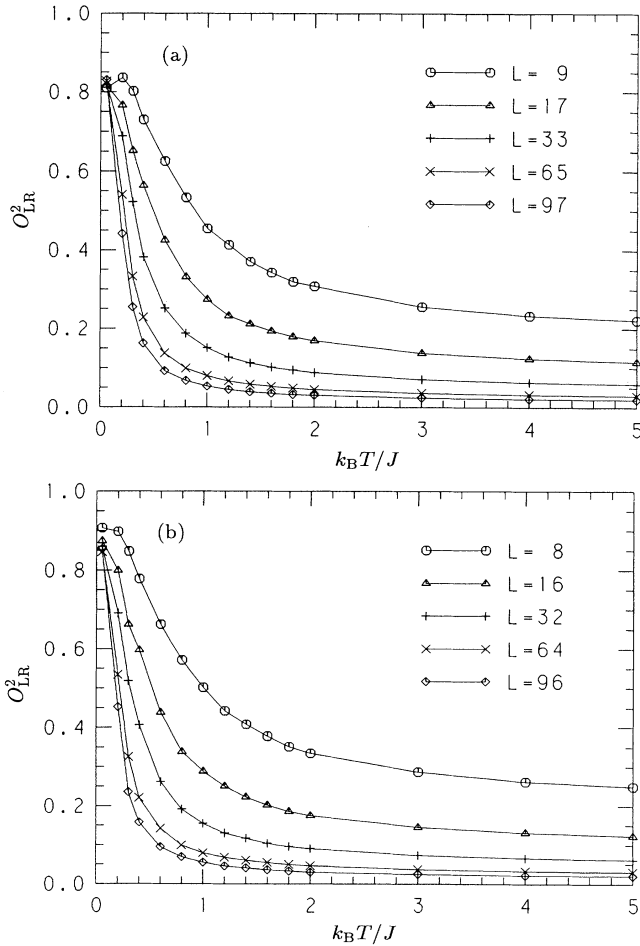


FIG. 9. Temperature dependences of the square of the nonlocal (long-range) hidden order parameter in open chains with odd numbers of spins (a) and periodic chains (b). Here the data at  $k_B T/J=0.05$  have been estimated through Eqs. (27) and (28), using the corresponding values obtained in the canonical ensemble where the total magnetization  $M_z$  is fixed.

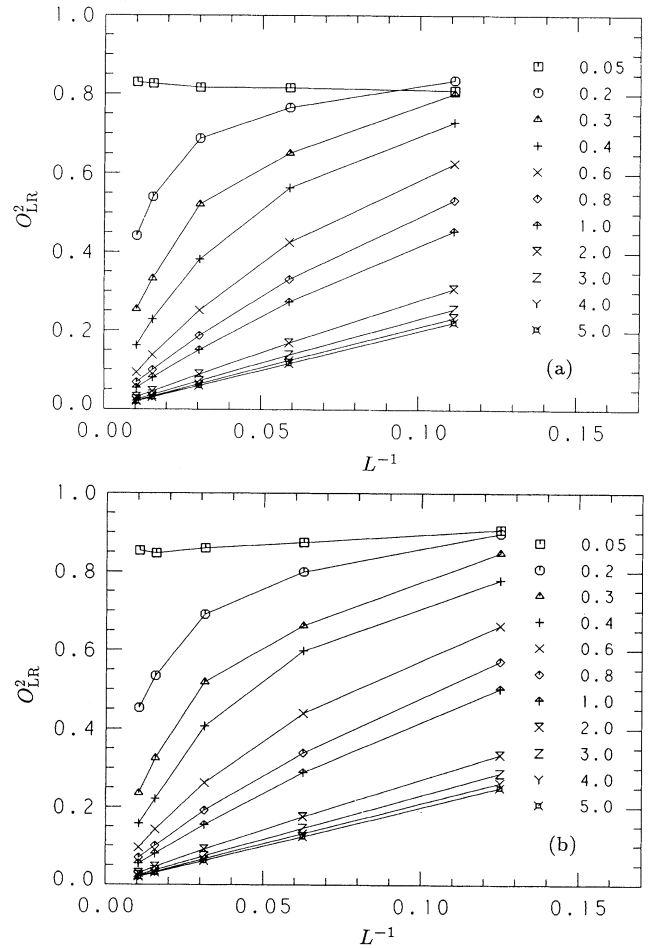


FIG. 10. Size dependences of the square of the nonlocal (long-range) hidden order parameter in open chains (a) and periodic chains (b). Here the data at  $k_B T/J=0.05$  have been estimated through Eqs. (27) and (28), using the corresponding values obtained in the canonical ensemble where the total magnetization  $M_z$  is fixed.



$\langle O_{\text{LR}}^2 \rangle$  at given temperatures in open odd chains (a) and periodic chains (b). At temperatures  $k_B T \geq 0.2$ ,  $\langle O_{\text{LR}}^2 \rangle$  approaches zero for large  $L$  as we see in Eq. (24). The temperature dependence of  $\xi_D$  is estimated from the size dependence. Here we have actually estimated the values of  $\xi_D$  from the slopes of the extrapolated curves at  $L \rightarrow \infty$  in Fig. 10. This estimation becomes less precise as  $\xi_D$  approaches the maximal length that we have investigated. On the other hand, if we assumed that the domain walls occur independently with the probability  $P_{\text{DW}}$  (22) at each pair, it would be expected that

$$\xi_D^{-1} = -\ln(1 - P_{\text{DW}}) = -\ln \left[ \frac{1 + O_{\text{SR}}}{2} \right]. \quad (25)$$

We plot in Fig. 11 the temperature dependence of the observed  $\xi_D$  and  $\xi_D^{-1}$  in the thermodynamic limit estimated through Fig. 10(a) and Eq. (24) ( $\blacktriangle$  and  $\bullet$ ), together with the corresponding values obtained from Eq. (25) using the data shown in Fig. 8(a) ( $\triangle$  and  $\circ$ ). We find that there is a qualitative difference between the two estimates at low temperatures. As  $T \rightarrow 0$ , the observed  $\xi_D^{-1}$  converges to zero, while the  $\xi_D^{-1}$  obtained through Eq. (25) remains finite. At  $k_B T/J = 0.05$ , which is low enough to represent the ground state,  $\langle O_{\text{SR}} \rangle \simeq 0.91$  in the chain with  $L = 97$  [Fig. 8(a)] and we then obtain from Eq. (25)  $\xi_D \simeq 22$  as plotted in Fig. 11. However, in Fig. 10(a),  $\langle O_{\text{LR}}^2 \rangle$  stays constant even in the long chains with  $L \gg 22$ . On the other hand, the correlation length  $\xi_D$  has been also investigated by a quantum transfer-matrix method<sup>29</sup> and we have confirmed that our observed  $\xi_D$  gives very good agreement with that result. From all these results, it is concluded that at low temperatures, the assumption of the independent appearance of the domain walls is wrong and the domain walls appear correlatively. We can observe this fact in Fig. 7, where the domains with the antiphase, which is opposite to the background phase, are localized in the world of space and time (the chain and the Trotter directions). These domains are

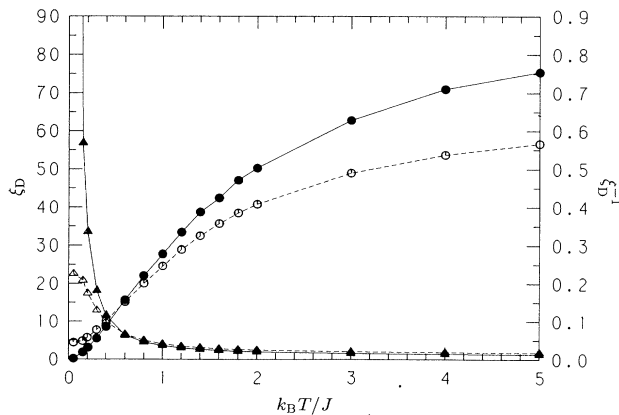


FIG. 11. Temperature dependences of the correlation length of the domain in the hidden ordering,  $\xi_D$ , and  $\xi_D^{-1}$  in the thermodynamic limit obtained from Fig. 10(a) and Eq. (24) ( $\blacktriangle$  and  $\bullet$ ) and through Eq. (25) ( $\triangle$  and  $\circ$ ).

nothing but quantum fluctuations that are not observed in the ground state of the AKLT model.

At  $T=0$  the spin configuration fluctuates through the off-diagonal operator  $S_i^+ S_{i+1}^- + S_i^- S_{i+1}^+$ , conserving the total magnetization. Quantum fluctuations of this type have no serious effect on the string order. We schematically show in Fig. 12 typical fluctuations of two types caused by the operator  $S_i^+ S_{i+1}^- + S_i^- S_{i+1}^+$ . In Fig. 12(a) the fluctuation does not affect the hidden order at all. In Fig. 12(b) the domain walls are produced in pairs but they destroy the hidden order only locally. Although the quantum fluctuations due to the operator  $S_i^+ S_{i+1}^- + S_i^- S_{i+1}^+$  reduce the magnitude of the long-range-order parameter, they do not destroy the hidden  $Z_2 \times Z_2$  symmetry breaking which has been discussed in the AKLT model.<sup>13</sup>

On the other hand, at finite temperatures the total magnetization fluctuates. In a Monte Carlo simulation these fluctuations are created by the global flip. Thus at  $T \neq 0$ , a single spin can flip [Fig. 12(c)]. Fluctuations of this type create an isolated domain wall and as a result the string order is destroyed nonlocally. In order to consider the intrinsic correlation in the string order, we should consider the probability of the appearance of the isolated domain wall  $P_{\text{IDW}}$  instead of  $P_{\text{DW}}$ . It is rather difficult to estimate  $P_{\text{IDW}}$  directly from the Monte Carlo simulation.  $P_{\text{IDW}}$  is estimated from the correlation length  $\xi_D$  as

$$\xi_D^{-1} = -\ln(1 - P_{\text{IDW}}). \quad (26)$$

Consequently, as the temperature approaches zero,  $P_{\text{IDW}}$  goes to zero, while  $P_{\text{DW}}$  remains finite. We show in Fig. 13 a typical snapshot at  $k_B T/J = 0.4$  of the two-dimensional Ising system with the isolated domain walls.

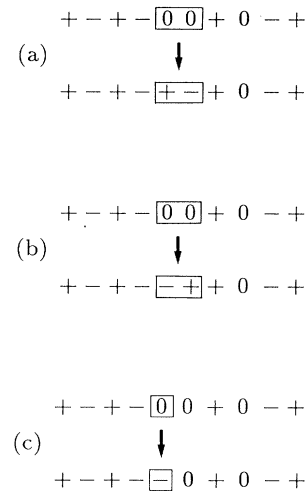


FIG. 12. Typical fluctuations of the spin configuration caused by the operator  $S_i^+ S_{i+1}^- + S_i^- S_{i+1}^+$  [(a) and (b)] and by allowing the total magnetization  $M_z$  to change (c). The fluctuation (a) does not affect the hidden order at all, (b) destroys the hidden order only locally, and (c) destroys the hidden order nonlocally.

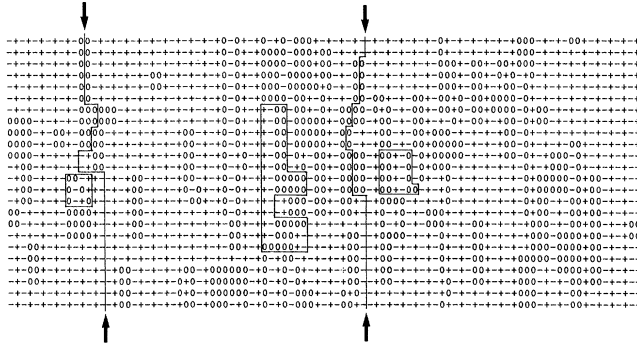


FIG. 13. A snapshot of the transformed two-dimensional Ising system at  $k_B T/J = 0.4$  on which a Monte Carlo simulation is being performed, where the horizontal and vertical lines denote the chain and Trotter directions corresponding to space and time, respectively.

Finally, we would like to point out that both  $O_{SR}$  and  $O_{LR}$  do depend on the value of the total magnetization  $M_z$ . In Fig. 14 the temperature dependences of  $\langle O_{SR} \rangle$  in the subspaces with  $M_z = 0$  and 1 are shown compared with the data obtained in the ground canonical ensemble where  $M_z$  is allowed to fluctuate. Since at  $k_B T/J = 0.05M_z$  scarcely fluctuates, we have performed the simulations in the subspaces with a fixed  $M_z$ . When we need the thermodynamically averaged values at very low temperatures, they can be obtained by averaging over the lowest energy levels; for example, as follows:

$$\langle O_{SR} \rangle = \frac{1}{4} [2\langle O_{SR}(M_z=0) \rangle + 2\langle O_{SR}(M_z=1) \rangle], \quad (27)$$

for open chains and

$$\langle O_{SR} \rangle = \langle O_{SR}(M_z=0) \rangle, \quad (28)$$

for periodic chains. Actually, these obtained approxi-

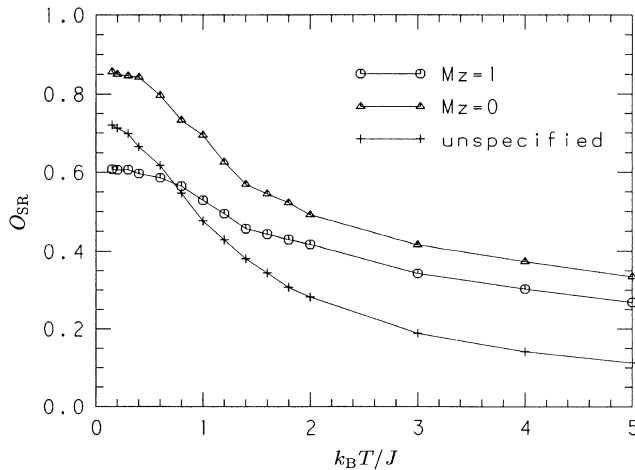


FIG. 14. Temperature dependences of the local hidden order parameter in the open chain with  $L=9$  obtained in the subspaces with  $M_z=0$  and 1 and in the ground canonical ensemble where  $M_z$  is allowed to fluctuate.

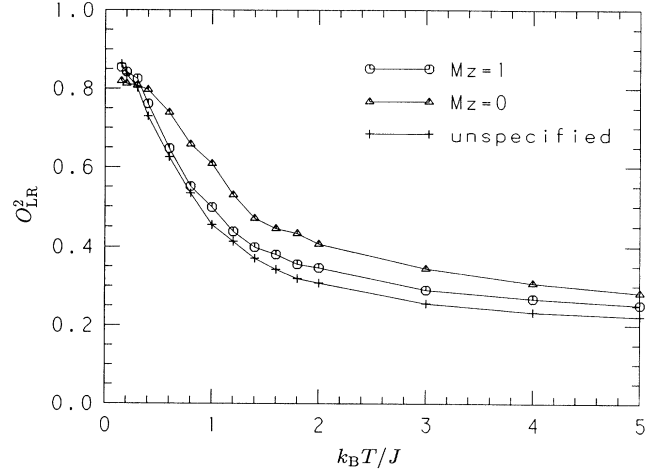


FIG. 15. Temperature dependences of the square of the non-local hidden order parameter in the open chain with  $L=9$  in the subspaces with  $M_z=0$  and 1 and in the ground canonical ensemble where  $M_z$  is allowed to fluctuate.

mate values give smooth extrapolations in Fig. 8. Of course, the difference between the values in the different subspaces becomes small as the chain length becomes large. We also show in Fig. 15 the  $M_z$  dependence of  $\langle O_{LR}^2 \rangle$  in the same manner as in Fig. 14. But the difference is rather small compared with the case of  $\langle O_{SR} \rangle$ .

## VI. SUMMARY AND DISCUSSION

Thermodynamic quantities of finite chains with free and periodic boundaries have been calculated by a quantum Monte Carlo method. We have investigated in detail the temperature dependences of the specific heat, the magnetic susceptibility, and the hidden order.

Regardless of the boundary condition, the peak of the specific heat is located at the temperature which is twice as much as the energy gap, although the shape of the specific heat is similar to the Schottky-type specific heat. It is also worth noting that the boundary condition has no significant effect on the behavior of the specific heat even in finite chains, where the structure of the low-lying energy levels changes according to the boundary condition. Thus we conclude that the temperature dependence of the specific heat in the present model should not be attributed simply to the energy gap between the ground state and the first excited state. This fact should be taken into consideration when the coupling constant of a sample described by the present model is estimated making use of the experimentally observed specific heat of the sample.

At low temperatures, the magnetic susceptibility in open chains, regardless of the number of spins in the chain, shows a Curie-like divergence whose amplitude is consistent with the two magnetic moments of  $S = \frac{1}{2}$  in the boundaries. This divergence is quantitative evidence of the appearance of two effective spin  $\frac{1}{2}$ 's induced in the boundaries which have been visualized in several theoret-

ical works.<sup>17,18</sup> Making use of the above result, we can estimate the number of open chains in a sample experimentally. In fact, the diverging behavior of the magnetic susceptibility has been already reported.<sup>23</sup>

Effects of anisotropy and an external field on the specific heat and the magnetic susceptibility are future subjects of great interest. For example, how does the magnetic field affect the temperature dependence of the specific heat? How does the single-ion anisotropy affect the amplitude of the Curie-like divergence of the magnetic susceptibility in open chains. These subjects will be reported elsewhere.

Although the present model has a quantum mechanically disordered ground state and the spin-correlation function decays exponentially, a long-range hidden order is detected in the ground state. Thus we have introduced the local (short-range) and nonlocal (long-range) hidden order parameters,  $O_{SR}$  and  $O_{LR}$ , and have investigated how the order develops as  $T \rightarrow 0$ . Both  $\langle O_{SR} \rangle$  and  $\langle O_{LR} \rangle$  become large as  $T \rightarrow 0$ , but neither of them take a perfect value even at  $T=0$  due to quantum fluctuations, in contrast with the case of the AKLT model. However, here we stress that the nonlocal hidden order detected by  $O_{LR}$  is not essentially destroyed by fluctuations at  $T=0$ . In other words, quantum-mechanical fluctuations are necessarily localized in the world of space and time (Fig. 7) and do not play an important role in destroying the long-range hidden order [Figs. 12(a) and 12(b)]. Thus we have estimated the intrinsic correlation length  $\xi_D$  in the model, namely, the correlation length of the hidden ordering, which diverges as  $T \rightarrow 0$ . We have studied the physical mechanism that causes the collapse of the hidden order at finite temperatures, making use of snapshots of the transformed two-dimensional Ising system (Fig. 13). The hidden order is nonlocally destroyed by an appearance of the isolated domain wall in the hidden ordering [Fig. 12(c)]. The isolated domain wall is created by changing the spin-projection value as  $\pm 1 \leftrightarrow 0$ . This appearance of the isolated domain wall by a single spin flip

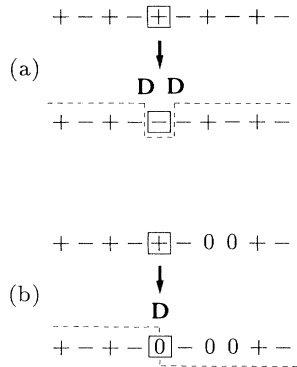


FIG. 16. Flips of a single spin in (a) an  $S=\frac{1}{2}$  antiferromagnetic chain, where  $\pm$  denote the spin projection  $\pm\frac{1}{2}$ , and in (b) an  $S=1$  antiferromagnetic chain, where  $\pm$  denote the spin projection  $\pm 1$ . The label  $D$  indicates the domain wall in the ordering.

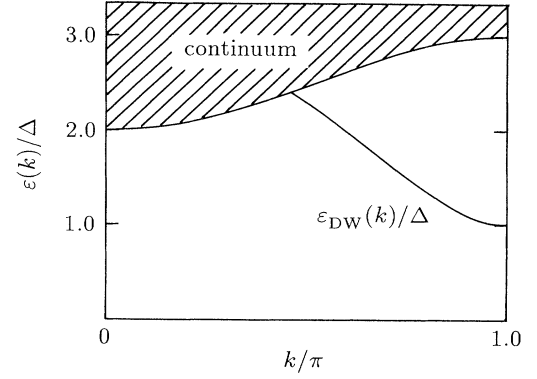


FIG. 17. An illustration of the energy dispersion relation expected in a material which shows the Haldane phase.

is characteristic of the present model. In the staggered ordering of spin  $\frac{1}{2}$ , a single spin flip creates two combined domain walls as shown in Fig. 16(a), where  $\pm$  denote the spin projection  $\pm\frac{1}{2}$ . The domain walls in Fig. 16(a) are nothing but a couple of spin waves in an  $S=\frac{1}{2}$  antiferromagnetic chain. Actually, Ishimura and Shiba pointed out<sup>30</sup> that two spin waves cause a continuum in the energy spectrum,  $\epsilon(k) = \epsilon_{DW}^{IS}(k') + \epsilon_{DW}^{IS}(k-k')$ , in an antiferromagnetic chain with  $S=\frac{1}{2}$ , where  $\epsilon_{DW}^{IS}(k)$  is the energy dispersion relation of a magnon. On the other hand, in the present model, a single spin flip creates an isolated domain wall shown in Fig. 16(b), which is an intrinsic fluctuation to destroy the hidden order, where  $\pm$  denote the spin projection  $\pm 1$ . Thus we can regard the isolated domain wall as an intrinsic excitation in the present model. In fact, an isolated branch in the dispersion relation has been recently observed<sup>31</sup> by neutron-scattering measurements in a material which shows the Haldane phase. This isolated branch separated from the continuum could be attributed to a neutron-scattering-induced isolated domain wall. Thus the system may have an isolated dispersion branch  $\epsilon_{DW}(k)$  which has a gap  $\Delta$  at  $k=\pi$ . For small  $k$ , there may be the continuum,  $\epsilon(k) = \epsilon_{DW}(k') + \epsilon_{DW}(k-k')$  starting from  $\epsilon(0)=2\Delta$ . Therefore, we expect the dispersion relation illustrated in Fig. 17. Recently, a similar structure of the energy spectrum has been proposed in studying the low-lying energy states of the present model by a numerical renormalization-group method.<sup>32</sup> The quantitative analysis of  $\epsilon_{DW}(k)$  is now under consideration.

#### ACKNOWLEDGMENTS

The authors would like to thank Professor K. Kubo for furnishing his unpublished data and Professor M. Takahashi and Dr. T. Sakai for valuable discussions. The authors also appreciate Professor T. Goto and Dr. N. Fujiwara for informing us of the experimental study of the magnetic susceptibility. Furthermore, one of the au-

thors (S. Yamamoto) is grateful to Professor H. Fukutome for his continuous encouragement. Numerical calculations were performed on a FACOM VP2600 in Kyoto University. The present work is partly supported by a

Grant-in-Aid for Scientific Research on Priority Areas, Computational Physics as a New Frontier in Condensed Matter Research, and from the Ministry of Education, Science and Culture.

- <sup>1</sup>F. D. M. Haldane, Phys. Rev. Lett. **50**, 1153 (1983); Phys. Lett. **93A**, 464 (1983).
- <sup>2</sup>R. Botet and R. Julien, Phys. Rev. B **27**, 613 (1983); R. Botet, R. Julien, and M. Kolb, *ibid.* B **28**, 3914 (1983).
- <sup>3</sup>H. Betsuyaku, Phys. Rev. B **34**, 8125 (1986).
- <sup>4</sup>K. Kubo and S. Takada, J. Phys. Soc. Jpn. **55**, 438 (1986); R. M. Nightingale and H. W. J. Blöte, Phys. Rev. B **33**, 6545 (1986); M. Takahashi, Phys. Rev. Lett. **62**, 2313 (1989).
- <sup>5</sup>W. J. L. Buyers, R. M. Morra, R. L. Armstrong, M. J. Hogan, P. Gerlach, and K. Hirakawa, Phys. Rev. Lett. **56**, 371 (1986); K. Kakurai, M. Steiner, R. Pynn, and J. K. Kjems, J. Phys. Condens. Matter **3**, 715 (1991); Z. Tun, W. J. Buyers, A. Harrison, and J. A. Rayne, Phys. Rev. B **43**, 13 331 (1991).
- <sup>6</sup>J. P. Renard, M. Verdaguer, L. P. Regnault, W. A. C. Erkers, J. Rossat-Mignod, and W. G. Stirling, Europhys. Lett. **3**, 945 (1987); J. P. Renard, L. P. Regnault, and M. Verdaguer, J. Phys. (Paris) Colloq. **49**, C8-1425 (1988); M. Date and K. Kindou, Phys. Rev. Lett. **65**, 1659 (1990); Y. Ajiro, T. Goto, H. Kikuchi, T. Sakakibara, and T. Inami, *ibid.* **63**, 1424 (1989); M. Chiba, Y. Ajiro, H. Kikuchi, T. Kubo, and T. Morimoto, Phys. Rev. B **14**, 2838 (1991); **45**, 5119 (1982); K. Katsumata, H. Hori, T. Takeuchi, M. Date, M. Yamagishi, and J. P. Renard, Phys. Rev. Lett. **63**, 86 (1989); N. Fujiwara, T. Goto, S. Maegawa, and T. Kohmoto, Phys. Rev. B **45**, 7837 (1992).
- <sup>7</sup>M. Takahashi, Phys. Rev. B **38**, 5188 (1988); K. Nomura, *ibid.* **40**, 2421 (1989); S. Liang, Phys. Rev. Lett. **64**, 1597 (1990).
- <sup>8</sup>I. Affleck and E. H. Lieb, Lett. Math. Phys. **12**, 57 (1986).
- <sup>9</sup>I. Affleck, T. Kennedy, E. H. Lieb, and H. Tasaki, Phys. Rev. Lett. **59**, 799 (1987); Commun. Math. Phys. **115**, 477 (1988).
- <sup>10</sup>M. den Nijs and K. Rommelse, Phys. Rev. B **40**, 4709 (1989).
- <sup>11</sup>S. M. Girvin and D. Arovas, Phys. Scr. **T27**, 156 (1989); Y. Hatsugai and M. Kohmoto, Phys. Rev. B **44**, 11 789 (1991).
- <sup>12</sup>H. Tasaki, Phys. Rev. Lett. **66**, 798 (1991).
- <sup>13</sup>T. Kennedy and T. Tasaki, Phys. Rev. B **45**, 304 (1992); Commun. Math. Phys. **147**, 431 (1992).
- <sup>14</sup>H.-J. Mikeska, Europhys. Lett. **19**, 39 (1992).
- <sup>15</sup>T. Sakai (private communication).
- <sup>16</sup>T. Kennedy, J. Phys. Condens. Matter **2**, 5737 (1990).
- <sup>17</sup>S. Miyashita and S. Yamamoto, Phys. Rev. B **48**, 913 (1993).
- <sup>18</sup>S. R. White, Phys. Rev. Lett. **69**, 2863 (1992); Phys. Rev. B (to be published).
- <sup>19</sup>M. Hagiwara, K. Katsumata, I. Affleck, B. I. Halperin, and J. R. Renard, Phys. Rev. Lett. **65**, 3181 (1990); J. R. Renard, *ibid.* **65**, 3181 (1990); S. H. Glarum, S. Geshwind, K. M. Lee, M. L. Kaplan, and J. Michel, *ibid.* **67**, 1614 (1991); J. Michel, *ibid.* **67**, 1614 (1991).
- <sup>20</sup>H. W. J. Blöte, Physica **79B**, 427 (1975).
- <sup>21</sup>H. Betsuyaku and T. Yokota, Prog. Theor. Phys. **75**, 808 (1986).
- <sup>22</sup>K. Kubo (unpublished).
- <sup>23</sup>O. Avenel, J. Xu, J. S. Xia, M.-F. Xu, B. Andraka, T. Lang, P. L. Moyland, W. Ni, P. J. C. Signore, C. M. van Woerkens, E. D. Adams, G. G. Ihas, M. W. Meisel, S. E. Nagler, N. S. Sullivan, Y. Takano, D. R. Talham, T. Goto, and N. Fujiwara, Phys. Rev. B **46**, 8655 (1992).
- <sup>24</sup>M. Suzuki, Prog. Theor. Phys. **56**, 1454 (1976).
- <sup>25</sup>J. E. Hirsch, R. L. Sugar, D. J. Scalapino, and Blankenbecler, Phys. Rev. B **26**, 5033 (1982).
- <sup>26</sup>A. Wiesler, Phys. Lett. **89A**, 359 (1982).
- <sup>27</sup>M. Suzuki, S. Miyashita, and A. Kuroda, Prog. Theor. Phys. **58**, 1377 (1977).
- <sup>28</sup>S. Takada, J. Phys. Soc. Jpn. **61**, 428 (1992); K. Hida and S. Takada, *ibid.* **61**, 1879 (1992).
- <sup>29</sup>K. Kubo, Phys. Rev. B **46**, 866 (1992).
- <sup>30</sup>N. Ishimura and H. Shiba, Prog. Theor. Phys. **63**, 743 (1980).
- <sup>31</sup>S. Ma, C. Broholm, D. H. Reich, B. J. Sternlieb, and R. W. Erwin, Phys. Rev. Lett. **67**, 3571 (1993).
- <sup>32</sup>S. R. White and D. A. Huse, Phys. Rev. B **48**, 3844 (1993).